Laser and Particle Beams (2008), *26*, 555–565. Printed in the USA.

doi:10.1017/S0263034608000591

Angular distributions of ions emitted from laser plasma produced at various irradiation angles and laser intensities

L. LÁSKA,[1] K. JUNGWIRTH,[1] J. KRÁSA,[1] E. KROUSKÝ,[1] M. PFEIFER,[1] K. ROHLENA,[1] A. VELYHAN,[1] J. ULLSCHMIED,[2] S. GAMMINO,[3] L. TORRISI,[3] J. BADZIAK,[4] P. PARYS,[4] M. ROSINSKI,[4] L. RYĆ,[4] AND J. WOLOWSKI[4]

[1]Institute of Physics, ASCR v.v.i., Prague, Czech Republic
[2]Institute of Plasma Physics, ASCR v.v.i., Prague, Czech Republic
[3]INFN, Laboratori Nazionali del Sud, Catania, Italy
[4]Institute of Plasma Physics and Laser Microfusion, Warsaw, Poland

(RECEIVED 28 May 2008; ACCEPTED 24 July 2008)

Abstract

Angular distributions of currents and velocities (energies) of ions produced at various target irradiation angles and laser intensities ranged from 10^{10} W/cm^2 to 10^{17} W/cm^2 were analyzed. It was confirmed that for low laser intensities the ion current distributions are always peaked along the target normal. However, at laser intensities comparable to or higher than 10^{14} W/cm^2, the preferred direction of ion emission strongly depends on the irradiation geometry (laser focus setting, the irradiation angle), and can be off the target normal. This is very likely caused by the non-linear interaction of the laser beam with produced plasma, in particular, by the action of ponderomotive forces and the laser beam self-focusing.

Keywords: Angular distribution; Ion emission; Irradiation angle; Laser-produced plasma

INTRODUCTION

A growing interest in the laser ion sources (LIS) in recent years has been based on their ability to produce ions with a broad spectrum of charge states (even higher than 50+) and with the kinetic energy in the MeV range. Moreover, they give extremely high ion current densities, which may attain values of hundreds of mA/cm^2 in the far expansion zone (~1 m) (Haseroth & Hora, 1996; Wolowski *et al.*, 2006, 2007; Badziak, 2007). There are various factors that influence characteristics and amount of emitted ions more or less (Láska *et al.*, 2007*a*, 2007*b*). These are the laser wavelength, the laser intensity, the focus setting, the angle of target irradiation, and the target surface properties. Very important is the focus position (FP) with regard to the target surface, because it determines not only the nominal laser intensity due to the caustic of the focused laser beam, but also the length- and time-scale of the interaction of the laser pulse with the preformed plasma (Láska *et al.*, 2004*a*, 2007*a*).

Address correspondence and reprint request to: L. Láska, Institute of Physics, ASCR v.v.i., Na Slovance 2, 182 21 Prague 8, Czech Republic. E-mail: laska@fzu.cz

At intensities above $\sim 1 \times 10^{14}$ W/cm^2, the optimum FP makes the interaction of the laser radiation with the expanding plasma plume very effective and the conditions for occurrence of various non-linear processes (including ponderomotive and/or relativistic self-focusing (Hora, 1969, 1975; Hauser *et al.*, 1992; Kumar *et al.*, 2006; Láska *et al.*, 2006; Rowlands, 2006)) can be met. Then heavy ions with the highest charge states and energy can be generated (Láska *et al.*, 2003, 2004*b*, 2005*a*). The necessary preformed plasma can be produced either by a suitable pre-pulse, preceding the main laser pulse, or due to the interaction of the front part of a sufficiently long main pulse (>100 ps), the rest of which interacts with the self-created plasma. Considering that ion generation starts at a laser intensity of $\sim 10^9$ W/cm^2, short (i.e., ps and sub-ps) laser pulses interact with the pre-formed plasma, too, because of their much longer (nanosecond) background. Moreover, the intensity contrast of the main pulse related to that background is usually not good enough (Rus *et al.*, 1997; Láska *et al.*, 2002*a*, 2004*a*, 2005*b*, 2007*a*; Badziak *et al.*, 2007). The essence of the optimum position of the focus in front of the target surface has already been found (Láska *et al.*, 1994; Woryna *et al.*, 1996*a*), various asymmetric dependencies with regard to the position of nominal maximum laser intensity, observed later (Láska *et al.*, 2005*c*, 2007*a*; Kasperczuk *et al.*, 2008), as well as the step in the dependence (Gitomer *et al.*, 1986, Fig. 4) can also be explained taking into account the interaction of the laser beam with the pre-formed plasma.

A lot of work has been invested on this topic, however, "there are still many questions with regard to the physics of the acceleration processes of these sources, and it is vital to understand in detail the dependence of the different acceleration mechanisms on the laser and target conditions" (Krushelnik *et al.*, 2005). This contribution presents some earlier results, yet unpublished (in this form, at least), and more recent ones that are concentrated mainly on the angular distribution of emitted ions and on the influence of the target irradiation angle.

EXPERIMENTAL ARRANGEMENT

The Nd:YAG laser LAB 100 at INFN-LNS in Catania, with the nominal energy of 900 mJ in 9 ns pulse duration was used for experiments at low laser intensities (10^{10} W/cm^2). With a lens of focal length $f = 500$ mm, the laser beam was focused onto a target of various elements located in the target chamber evacuated to $\sim 10^{-7}$ mbar. The minimum focus diameter was below 1 mm. The position of target chamber flanges (17°, 30°, 43°, and 56°) with regard to the laser input window, together with the rotating movable target holder made the measuring of the angular distribution of an ion emission possible (Torrisi *et al.*, 2000, 2001*a*, 2001*b*; Láska *et al.*, 2002*b*).

The laser intensities above 10^{16} W/cm^2 were delivered onto the target by a high-power iodine laser system PALS ($\lambda = 1.315$ µm, $E_L \leq 1$ kJ, $\tau \leq 350$ ps, $I_L \leq 6 \times 10^{16}$ W/cm^2, possible conversion to 2ω and 3ω) at the PALS Research Centre in Prague (Jungwirth *et al.*, 2001; Jungwirth, 2005). Solid targets were irradiated either perpendicularly or at 30° with respect to the target normal. The laser beam was focused with an aspheric lens ($f = 627$ mm for 1ω and $f = 600$ mm for 3ω) onto targets with a minimum focus spot diameter of ~ 70 µm. The ICs were positioned inside the target chamber (Wolowski *et al.*, 2002*a*). The data obtained in earlier experiments, employing an iodine laser system PERUN (Láska *et al.*, 1996), completed the new experimental data. The positions of output windows of the smaller PERUN chamber were located at 40° (IC), 60° (S1), and 90° (S2) with regard to the laser beam (Woryna *et al.*, 1999) as shown in Figure 1.

In addition, a picosecond (sub-nanosecond) Nd:glass laser at the Institute of Physics and Laser Microfusion in Warsaw ($\lambda = 1.05$ µm, $E_L \leq 1$ J, $\tau \leq 1$ ps, $I_L \leq 1 \times 10^{17}$ W/cm^2 (Wolowski *et al.*, 2002*b*; Badziak *et al.*, 2003, 2004) was used for short pulse experiments. The laser beam was focused onto a target by a parabolic mirror with a small

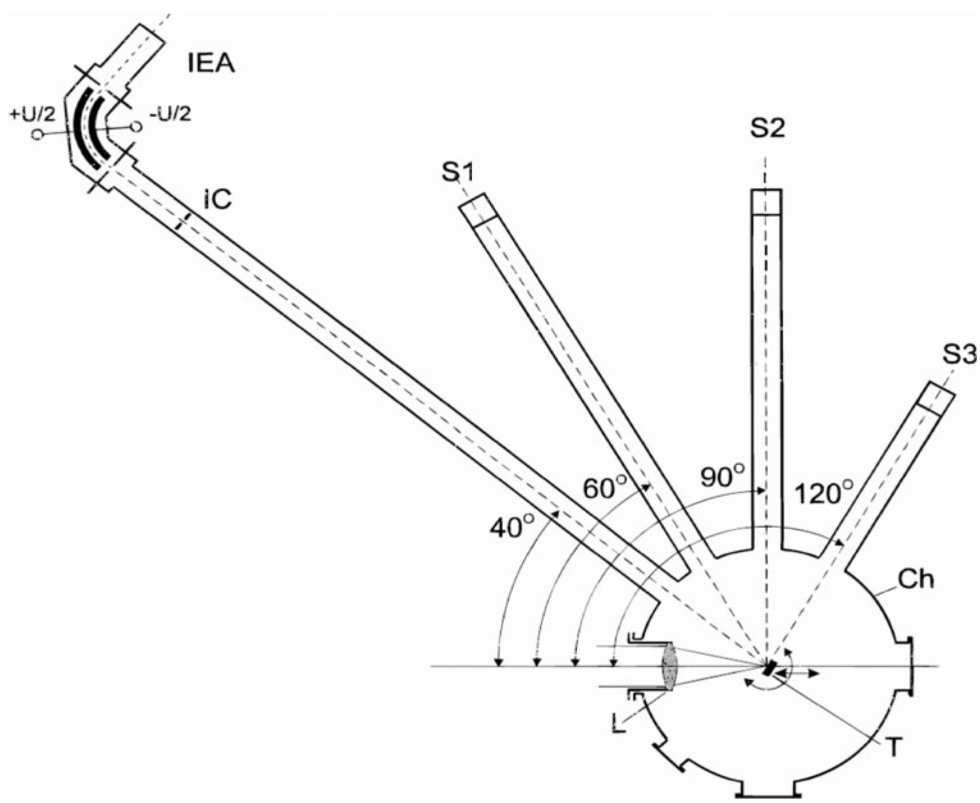

Fig. 1. Scheme of the PERUN target chamber (CH – Target Chamber, L – Focusing Lens, T – Target Holder, IEA, IC, S1, S2, S3 – ICs).

https://doi.org/10.1017/S0263034608000591 Published online by Cambridge University Press

hole in its center. The advantage of this mirror is a possibility to irradiate the target and simultaneously to detect the emitted ions along the target normal.

The corpuscular diagnostics was based on the time-of-flight (TOF) method using various types of ICs and a cylindrical electrostatic ion energy analyzer (IEA) (Láska *et al.*, 1996; Woryna *et al.*, 1996*b*; Wolowski *et al.*, 2002*a*). Ions were detected in a far expansion zone (~1 m) where the three-body recombination collisions are negligible and the ion charge-states are "frozen" (Rohlena *et al.*, 1996). It is worth remembering that the appropriate critical length L_{cr} from the target was measured to be ~20 cm for the Cu ions produced by an excimer (XeCl) laser delivering low intensity (Lorusso *et al.*, 2005), and it is shorter than 80 cm for iodine laser delivering intensities about 10^{14} W cm^{-2} (Krása *et al.*, 1999). However, it was calculated to be even longer than 1 m for CO_2 laser (Roudskoy, 1996). A quadruple mass analyzer Quadstar 421 was used to investigate neutral species ejected from the target (Torrisi *et al.*, 2000, 2001*a*).

RESULTS AND DISCUSSION

Ions Produced at Low Laser Intensity

The laser beam, which is focused onto solid targets at low intensities, heats, melts, and evaporates the target material. Starting from some threshold intensity (~10^9 W/cm^2 for Nd:YAG), the ions in addition to a different kind of neutrals are emitted. The threshold laser energies and the laser energy fluences for the ion generation of various target elements (Al, Au, Cu, Nb, Ni, Pb, Sn, Ta, W) were investigated (Torrisi *et al.*, 2000, 2001*a*, 2001*b*). They are presented in Table 1 together with typical mean values of the velocity and kinetic energy of ions, corresponding to the ion current peaks, observed close to threshold intensities. The ion current densities were obtained using the relation:

$$j = \frac{U}{RST(1+\gamma z)}, \tag{1}$$

U is the output IC voltage, the load resistance $R = 25\ \Omega$, S is the IC area, T is the IC grid transmission, γ is the coefficient of secondary electron emission induced by the impact of ions on the IC electrode, and z is the charge-state of ions. Melting points and boiling points of tested elements are included in Table 1 for completeness.

The angular distribution of ions produced by 9-ns pulses of the Nd:YAG laser was assembled from values of peak ion-current densities (1) measured simultaneously in four positions of ICs and changing stepwise the target tilt angle from 10° to 69° with regard to the laser beam. The peak ion currents were normalized to the peak current observed along the target surface normal. In fact, we obtained four dependencies, differing in laser irradiation angle (17°, 30°, 43°, 56°), as well as shifted with regard to each other in the region of the recorded distribution angles. This variation in the target tilt angle θ also results in a decrease of the irradiating laser intensity according to cosθ. The angular distributions of peak ion currents, obtained at laser intensities of about 5×10^9 W/cm^2, are shown in Figures 2a–2i together with the fitted function

$$j_{BL} + j_{\max}\cos^p(\varphi - \varphi_0), \tag{2}$$

where j_{BL} is the base line of the measured TOF spectra $j_\varphi(t)$, $j_{\max}$ is the peak value of $j_\varphi(t)$, and φ_0 is the deviation from the target normal along with the main part of ions expands into the vacuum, as it is generally observed (Ehler, 1975). The shape of the angular distribution of ions was found to be independent of the angle of irradiation of the target up to 60°, in fact.

The fitted values of the exponent p and the corresponding widths (full width at half maximum, FWHM) of the measured angular distributions of ion currents shown in Figure 2 are the content of Table 1. The phenomenological description of the angular dependence of the peak ion-current is improved generally by an extension of Eq. 2 to $a_0 + a_1 \cos(\varphi - \varphi_0) + a_p \cos^p(\varphi - \varphi_0)$ – (two component structure) (Thum *et al.*, 1994; Woryna *et al.*, 2001). According to Buttini *et al.* (1998) and Thum-Jager and Rohr (1999), the exponent p should increase and FWHM should decrease with the increasing ion mass, A, approximately following $A^{1/2}$ or $A^{3/4}$ law, as it was observed for the total charge

Table 1. *Some typical characteristics of the tested elements and of the generated ions*

Element	E_{th} [mJ]	F_{th} [J/cm^2]	$<v>$ [cm/s]	$<E_i>$ [keV]	Melt.p. [°C]	Boil.p. [°C]	p	FWHM [deg]
$_{13}Al^{27}$	24	0.14	9×10^6	1.1	660	2450	4	51.1
$_{28}Ni^{59}$	24	0.52	6×10^6	1.1	1453	2730	5	47.2
$_{29}Cu^{64}$	19	0.17	5×10^6	0.83	1083	2595	21	24.9
$_{41}Nb^{93}$	16	1.00	4×10^6	0.77	2468	4742	23	23.7
$_{50}Sn^{119}$	31	0.72	3×10^6	0.56	232	2270	7	37.2
$_{73}Ta^{181}$	25	0.67	3×10^6	0.85	2996	5425	7	37.4
$_{74}W^{182}$	17	1.40	3×10^6	0.85	3410	5930	33	19.9
$_{79}Au^{197}$	25	0.16	3×10^6	0.92	1063	2970	10	31.9
$_{82}Pb^{207}$	25	0.60	2×10^6	0.43	327	1725	8	34.8

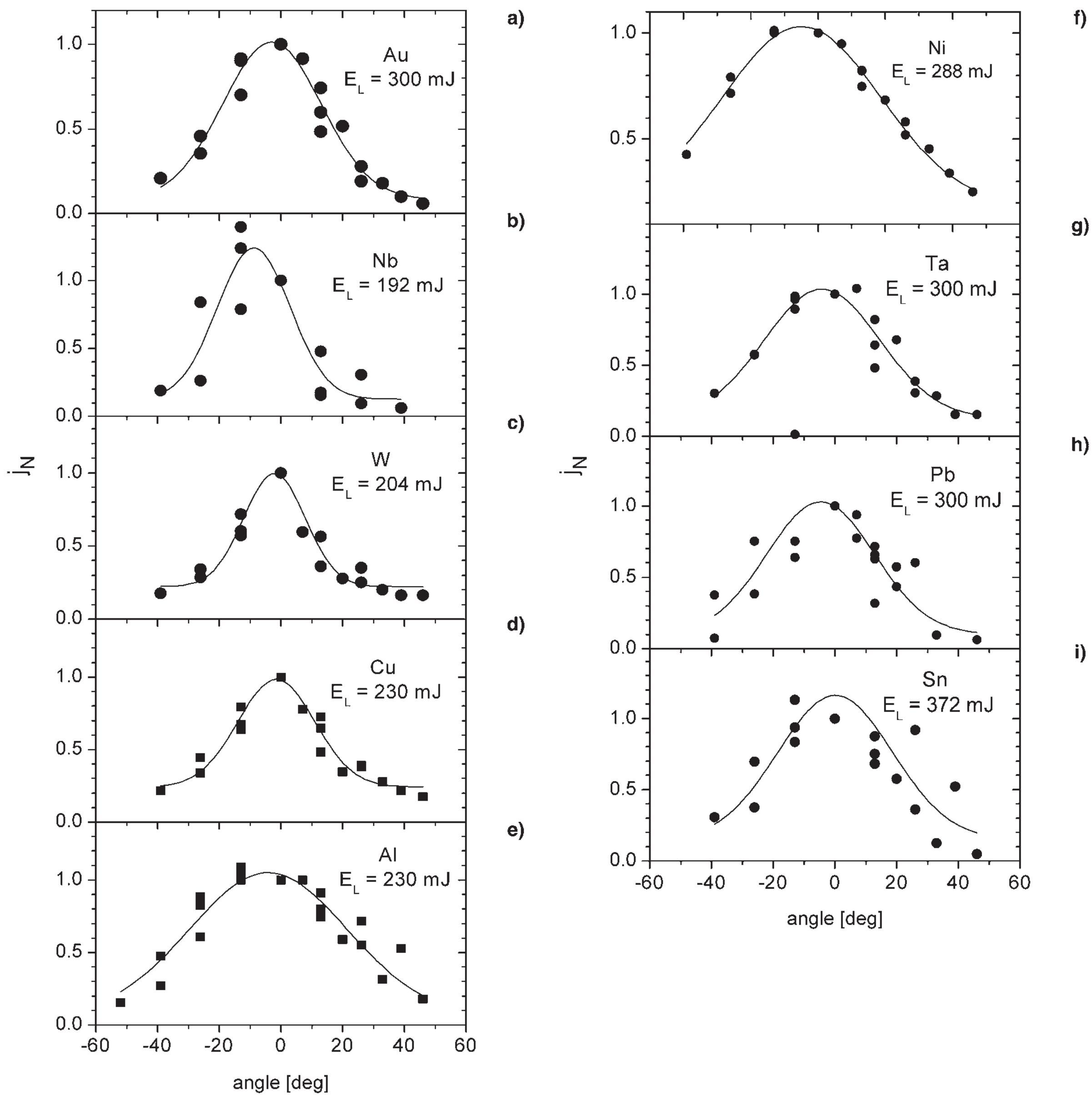

Fig. 2. Angular distributions of normalized current densities of emitted ions, j_N, produced by low laser-intensities, irradiating various target elements (for more details, see text).

emitted or the numbers of particular ion species, respectively. However, these atomic mass dependencies of the angular distribution observed for the peak ion-currents were not found completely confirmed. The broadest angular distribution of an ion current was observed for Al, the narrowest one for W.

Some additional questions are evoked in connection with the angular distribution of ions: what is the kind, number, and energy of single ions, emitted into different (chosen) angles with regard to the target normal (isotropy of ion-carried kinetic energy), and whether there are any differences and which one in ion characteristics, comparing ion expansion against (−) or in the direction (+) of radiation of the laser beam. The IC gives the time-resolved, but charge-integrated signal, $U(t) = R \quad i(t) = R \quad dQ/dt = R \quad d(N(t) <z(t)> e)/dt$, where $N(t)$ is the number of ions, $<z(t)>$ is the averaged charge-state of ions at the instant t, and e is the elementary charge. Since the measured ion current is a sum of particular currents of various ionized species, both magnitudes N and $<z>$ must be determined with the use of another kind of ion diagnostics such as a cylindrical IEA or Thomson parabola spectrograph (TPS) (Woryna *et al.*, 1996*b*), or the diagnostics can be completed by a numerical deconvolution of IC signal with more or less peaks or humps (Krása *et al.*, 2007; Picciotto *et al.*, 2006). The retrieval of the particular ion currents, produced by various mechanisms, makes the determination of the total

https://doi.org/10.1017/S0263034608000591 Published online by Cambridge University Press

number N of ions and their mean charge state $<z>$ possible. Then the integral of an IC signal, i.e., the value of the total charge of collected ions can be interpreted in the frame of the product $N<z>e$. Similarly, it is possible to determine experimentally the mean velocity $<v_i>$ and the total energy of expanding ions $E=<E_i>N$, where $<E_i>$ is the mean energy carried by a single ion. This simplest analysis of IC signals measured at different directions of the plasma expansion can contribute to elucidation of the phenomenological angular dependence represented by Eq. (2) or its expanded version. It is evident that the angular expansion of the plasma depends not only on the hydrodynamic properties of the plasma but also on the created ambipolar electric field, accelerating the ions mainly along the target normal (Krása *et al.*, 2007). Therefore, the above-mentioned effect of the ion mass on the value of FWHM should be completed by the angular distribution of centre-of-mass velocity of particular ion species.

The expansion of laser-produced plasma primarily depends on the velocity distribution of the expanding ion species (Stritzker *et al.*, 1981; Kelly & Dreyfus, 1988). As it was presented elsewhere (Krása *et al.*, 2008), the response of IC to an impacting ion current can be expressed in the form

$$j_{IC}(t) \propto v_x f(\vec{v}) d\vec{v} \propto \frac{L^2}{t^5} f\left(\frac{L}{t}\right), \tag{3}$$

where f is the velocity distribution, t is the TOF through the distance L. If a shifted Maxwell–Boltzmann velocity distribution describes the properties of the expanding fluid, then the IC signal is

$$j_{IC}(L,t) \propto t^{-5}\exp[-\beta^2(L/t-u)^2], \tag{4}$$

where $\beta^2 = m_i/2kT$ and u is the center-of-mass velocity. The peak velocity, i.e., the velocity corresponding to the maximum of a time-resolved ion current (TOF spectrum), is expressed by:

$$u_{peak} = \frac{1}{5}\sqrt{\frac{m}{2kT}}\left(\sqrt{10+\frac{mu^2}{2kT}} - \sqrt{\frac{mu^2}{2kT}}\right). \tag{5}$$

Since the ion current detected with an IC is composed of particular currents $j_{A,q}$ of a number of ion species having atomic mass A and charge-state q

$$j_{IC}(L,t) = \sum_{A,q} j_{A,q}(L,t) \tag{6}$$

Eq. (3) should be substituted in Eq. (5). Then the equation expressing the peak velocity of the total current would depend on the number of parameters relating to all the particular currents as the numbers of ion species, their center-of-mass velocities and the temperature. For simplicity Eq. (4) could help to elucidate the angular dependencies of peak velocities (energies) measured for various elements shown in Figure 3.

The center-of-mass velocity u, which is generally dependent on the accelerating ambipolar field and collisional rates of ions, significantly affects the peak velocity, as Eq. (4) suggests (Krása *et al.*, 2007). If the laser beam hits a target obliquely, then the plasma expanding along the target normal could interact with the laser beam only by its lateral part. Such interaction could result in acceleration of fast electrons along the laser-beam axis with a consequent increase in center-of-mass velocity u in the range of angle from -10° to -69°, as the target is rotated. The highest asymmetry in the angular distribution of peak velocities shows the Au-plasma (Fig. 3a). The maximum near the target normal, i.e., at 0°, was well distinguishable for Nb-, W-, Cu- and Al-plasmas, as Figures 3b to 3e show. The peak velocity of expanding Ni- and Ta-plasmas are nearly angular independent, see Figures 3f and 3g. A more complex dependence (decrease) in the peak velocity was observed for Pb- and Sn-plasmas, but a peak-velocity enhancement at about 30° can be hardly elucidated without invoking a formation of side jet-like plasma emission during the plasma production. For the precise description of this phenomenon, it would be necessary to determine the particular currents of all the emitted ion species or to retrieve these particular currents by a mathematical deconvolution method of IC signal, i.e., TOF spectrum, based on Eqs. (3) and (5) (Krása *et al.*, 2007, 2008).

It is worth remembering at this moment that the IC signal reflects the plasma production mechanisms, participating in the ion production (Láska *et al.*, 2005*a*, 2005*b*), and also influencing the direction of the ion expansion. The planar geometry of the target tends to emit ions due to the strong ambipolar electric field accelerating the ions perpendicularly to the target, while the radial component of the ponderomotive or thermo-kinetic forces drive them radially with regard to the laser beam axis.

Ions Produced by High Laser Intensity

Starting from the laser intensity of $\sim 10^{14}$ W/cm^2, non-linear processes in the pre-formed (pre-pulse) plasma support the generation of ions with the highest energy and the highest charge states (Láska *et al.*, 2004*a*, 2005*a*; Badziak *et al.*, 2007) (see Fig. 4). Also experiments of VanRompay *et al.* (1998) with the fs laser (10^{15} W/cm^2) and carbon target confirmed that the size, shape, and charge states of the ion energy distributions in the ablation plume depend strongly on the laser intensity, and even more importantly, on the laser pulse contrast. The presence of pre-pulse can significantly modify this distribution.

If ions with a high energy ($\sim$1 MeV) are generated in the laser plasma, directional maxima of ion emission other than normally to the target may appear in addition to the main ion peak. High-energy (0.15–4 MeV) fast phosphor ions produced at laser power densities $\sim 10^{15}$ W/cm^2, were

https://doi.org/10.1017/S0263034608000591 Published online by Cambridge University Press

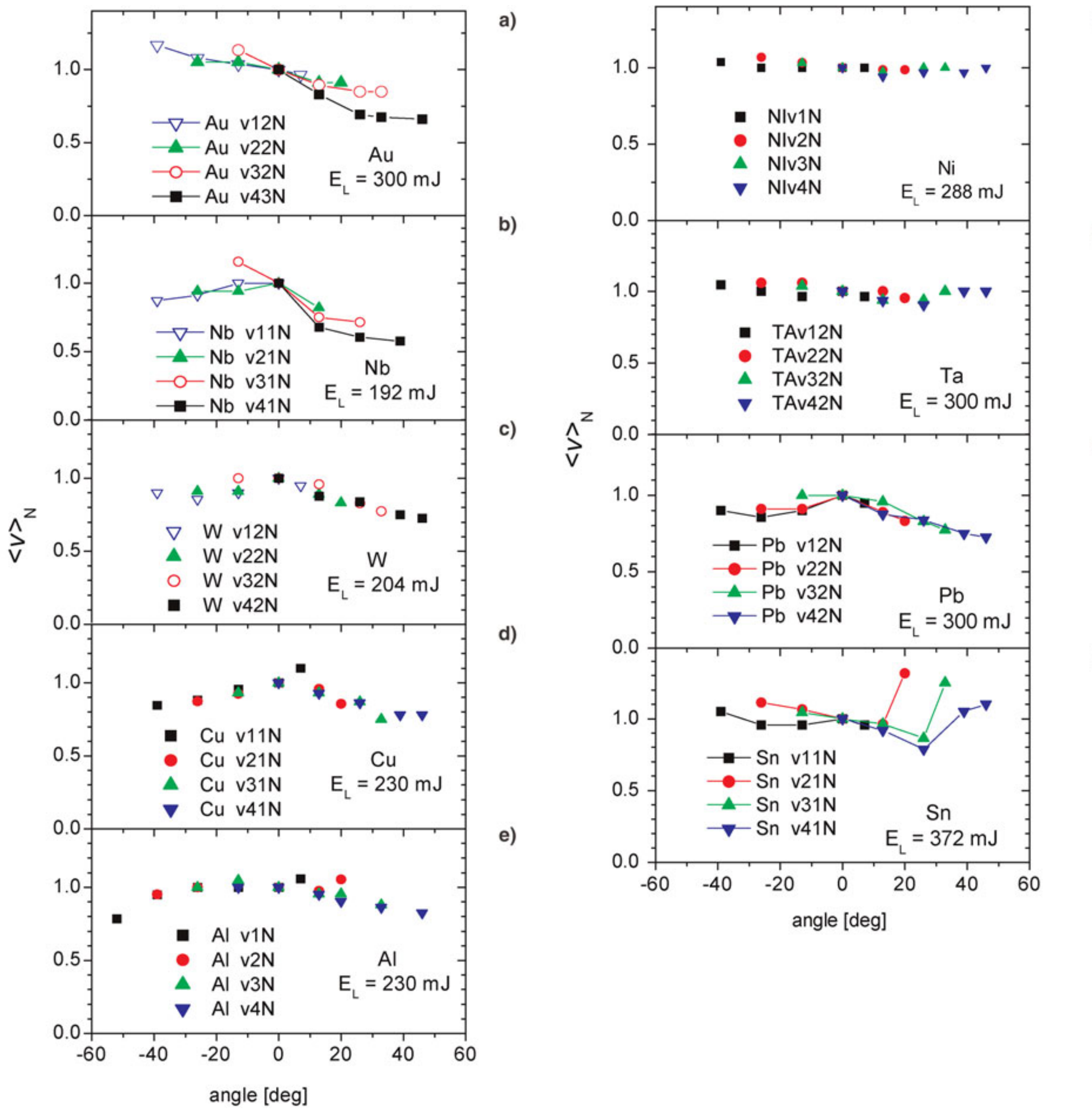

Fig. 3. (Color online) Angular distributions of the peak (mean) ion velocity $<v>$ (with respect to the target normal and corresponding to the Fig. 2).

found to be emitted almost parallel to the target surface by Basov *et al.* (1987). This fact was explained by the acceleration of ions due to the ponderomotive forces at relativistic self-focusing of the laser beam in the plasma (Hora, 1975; Hauser *et al.*, 1992). We observed a second maximum for Al ion velocities from 1×10^7 cm/s to 1×10^8 cm/s (energy up to 140 keV) at about 60° from the target normal (Chvojka *et al.*, 1994; Mróz *et al.*, 1994). (If the angular distribution is presented in the polar coordinates, an approximate form of expanding plasma plume is recovered due to the point-like source of ions.)

The PERUN laser (5×10^{14} W/cm^2) was used for more detailed studies of angular distribution of the emitted Au, Pb, and Sn ions (Woryna *et al.*, 1999). IC signals, measured at various angles, were normalized to the same distance of 144 cm according to the $j \sim L_{IC}^{-3}$ law. The velocity limit of 1×10^8 cm/s was postulated to define the slow and the fast ions. This separation also helps to determine the charge carried by both the ion groups. The IC signals were integrated over two TOF ranges, corresponding to the separate two ion groups mentioned. Figure 5 shows an example of the angular distribution of the charge density of the slow (energy lower than ~1 MeV, broken line) and fast (energy higher than ~1 MeV, full thin line) Au ion groups, determined in the above-mentioned way. The thick full line represents angular distribution of the total charge density, which is a sum of the partial distributions of both ion groups. In this case, the FP = −125 μm was in front of

https://doi.org/10.1017/S0263034608000591 Published online by Cambridge University Press

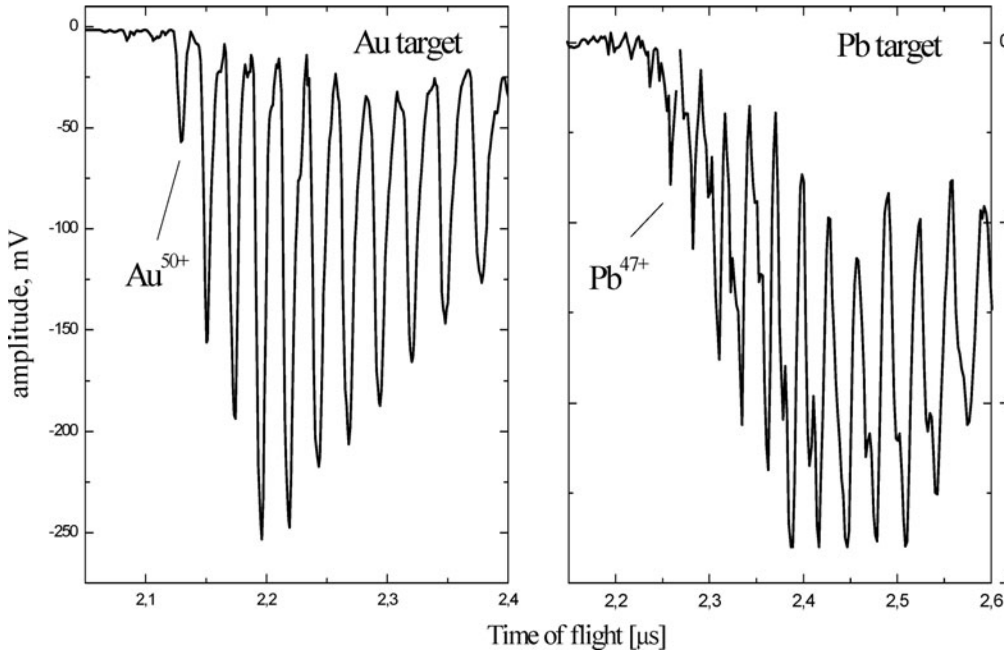

Fig. 4. Highly charged Au and Pb ions recorded by IEA (Au: 1ω, $E_L = 14.5$ J, $\varphi = 25°$, FP $= -125$ μm, $E/z = 20$ keV; Pb: 1ω, $E_L = 22.7$ J, $\varphi = 35°$, FP $= -100$ μm, $E/z = 20$ keV).

the target surface, and the target tilt angle φ was 40°. The preferred emission angle of slow ions is close to the target normal (about 40° to the laser beam), while it is about 20° with respect to the target normal (i.e., about 60° to the laser beam) for the fast ions. Preferred direction (angle) of total charge (the sum of both slow and fast groups) is within about 10° from the target normal (about 50° to the laser beam axis). Changing the target tilt angle from 20° to 45°, the preferred direction of emission of the slow ion group remains close to the target normal, while for the fast ion group the preferred emission angle decreases from ~40° to ~20° with respect to the target normal. Figure 6 shows an angular distribution of the total charge density of Au and Pb ions at various angles of target irradiation (tilt angle 20°–45°, see symbol labels in Fig. 6) and related to the IC position (40°). Considering the preferred emission angles of the total charge of both ion groups, they reflect the number (ratio) of the produced slow and fast ions, and, in fact, also a kind of prevailing mechanism of their generation and acceleration. The dependence of preferred emission angles of total ion charge on the target tilt angle is shown in Figure 7. However, the situation is more complex due to the dependence on laser FP, which significantly affects the ion production independently of the irradiation angle. This fact is clearly demonstrated for Au and Sn ions in Figure 8.

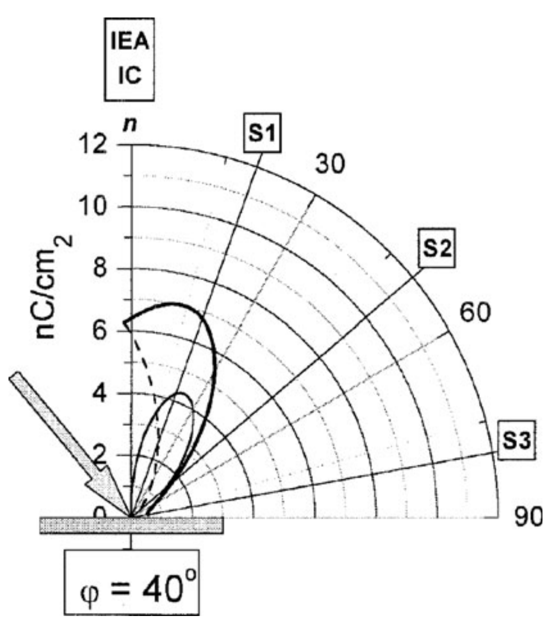

Fig. 5. Angular distribution of the charge density of slow (thin dotted line) and fast (thin full line) Au ions and of the total charge density (thick full line); 1ω, $E_L = 30$ J, $\varphi = 40°$, FP $= -125$ μm (for more details, see text).

Values of ion charge states up to ~57+ and peak ion energy ~30 MeV for Au and Ta ions were recorded by using the PALS laser system at intensities up to 5×10^{16} W/cm^2. The higher laser intensity, the larger preferred emission angle of the fast ion groups. Angular distributions of emitted Ta ions presented in Figure 9, all produced at laser frequency 3ω, were determined with ICs located inside the target chamber (Badziak *et al.*, 2004; Wolowski *et al.*, 2003, 2006) at short distances of ~50 cm from the target. Lower ion current densities (curve 1) were recorded at a target tilt (irradiation) angle of $\varphi = 30°$ ($E_L = 225$ J). Higher ion currents (curve 2) were measured at the perpendicular target irradiation ($\varphi = 0°$), in this case, $E_L = 140$ J only. The highest ion yield (curve 3) was recorded with the separate laser pre-pulse (~10 J) 4.6 ns before the main pulse, at the

https://doi.org/10.1017/S0263034608000591 Published online by Cambridge University Press

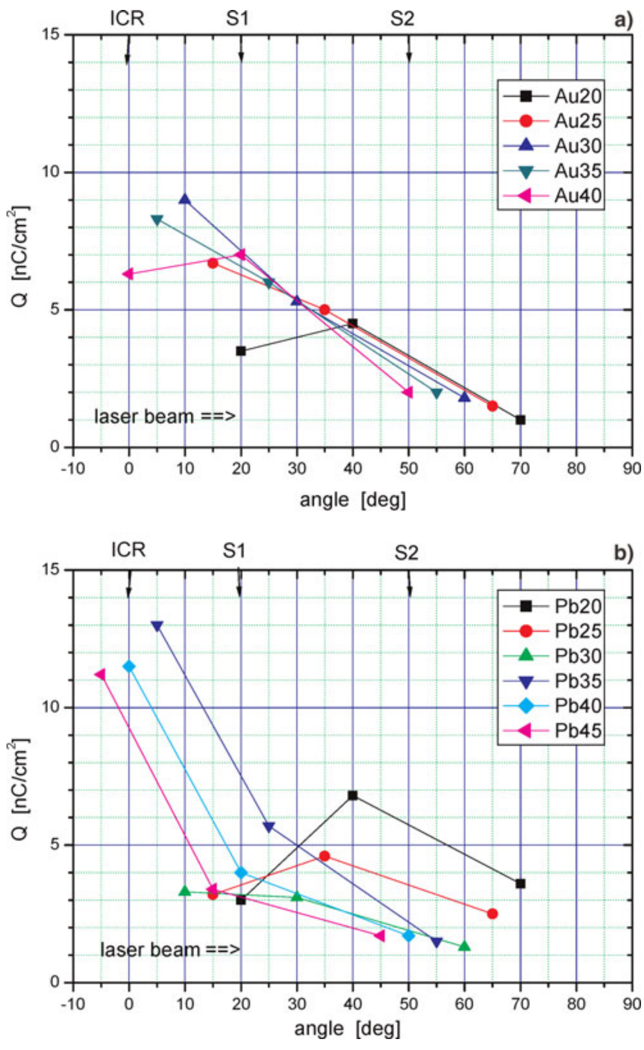

Fig. 6. (Color online) Angular distribution of the total charge density, Q, of Au (**a**) and Pb (**b**) ions at target tilt angles 20°–45° (Au: 3ω, $E_L = 30$ J, FP = −125 μm. Pb: 3ω, $E_L = 22$ J, FP = −20 μm).

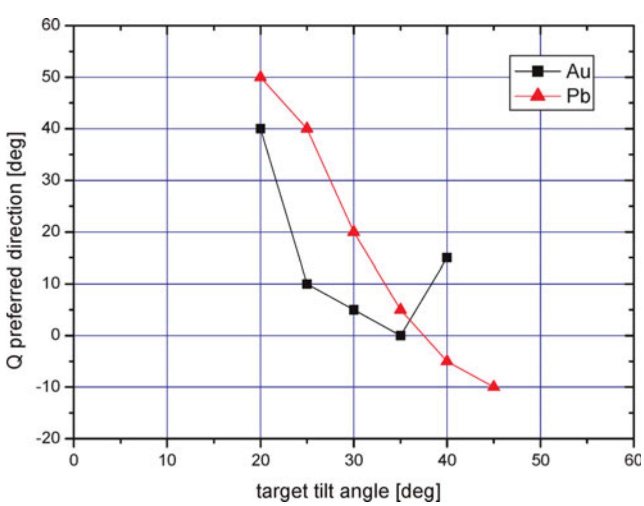

Fig. 7. (Color online) Preferred emission angles of the total charge, Q, of Au and Pb ions in dependence on the target tilt (irradiation) angle (Au: 3ω, $E_L =$ 30 J, FP = −125 μm. Pb: 3ω, $E_L = 22$ J, FP = −20 μm).

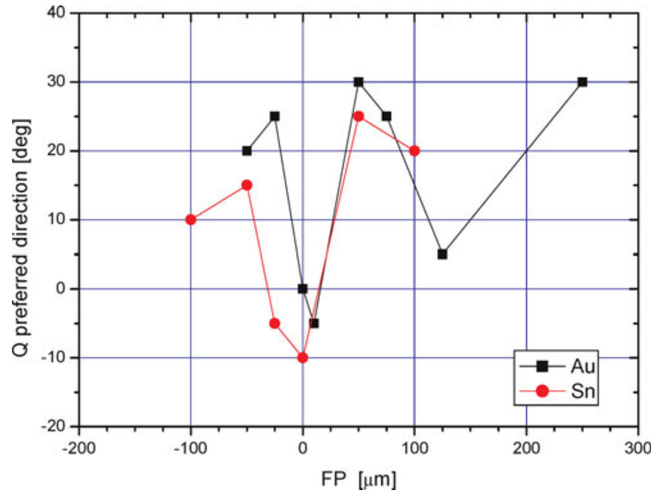

Fig. 8. (Color online) Preferred emission angles of the total charge, Q, of Au and Pb ions in dependence on the FP at fixed laser energy and irradiation angle (Au: 3ω, $E_L = 19$ J, $\varphi = 30°$. sn: 3ω, E_L= 24 J, $\varphi = 40°$).

same other experimental conditions. Significant effect of interaction of laser beam with the pre-formed plasma was also confirmed in different sns-pulse experiments by finding preferred emission maxima for Au ions at ∼24°, not perpendicular to the target surface (see Fig. 10). Angular distribution for ps pulse is included for a comparison (Wolowski *et al.*, 2002*b*; Badziak *et al.*, 2003, 2004).

The main part of the emitted ions in most of the experiments is reported along the target normal. This fact corresponds also to the results of systematic interferometric studies of plasma jets, emitted from the plasma of various target elements (Al, Au, Cu, Pb, Ta) (Schaumann *et al.*, 2005; Nicolai *et al.*, 2006; Kasperczuk *et al.*, 2006, 2007). Such plasma jets are about 200 μm in diameter (very

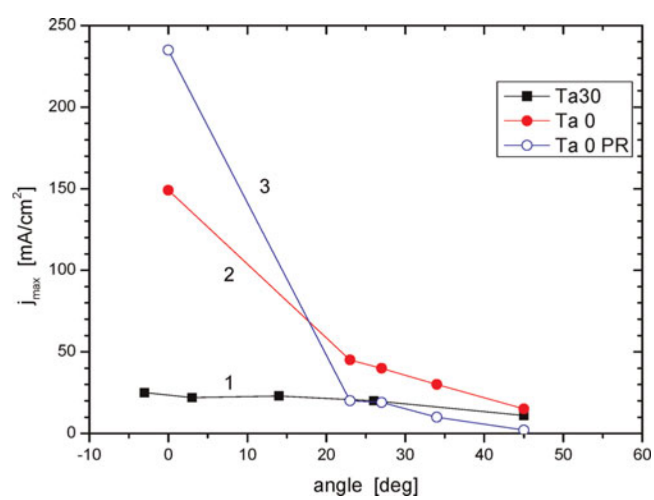

Fig. 9. (Color online) Angular distribution of the maximum at current density of Ta ions, j_{max}, recorded at high laser intensities (PALS) At three various irradiation conditions (1 – 3ω, $E_L = 225$ J, $\varphi = 30°$, FP = 0 μm; 2−3ω, $E_L = 140$ J, $\varphi = 0°$, FP = 0 μm; 3−3ω, $E_L = 140$ J, $\varphi = 0°$, FP = 0, 10 J pre-pulse 4.6 ns before the main pulse).

https://doi.org/10.1017/S0263034608000591 Published online by Cambridge University Press

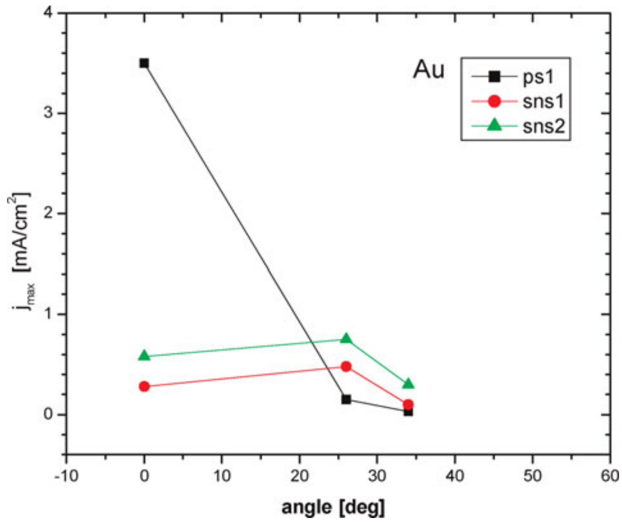

Fig. 10. (Color online) Angular distribution laser of the maximum current density of Au ions, j_{max}, produced by Nd:YAG laser, delivering picosecond (ps) and sub-nanosecond (s-ns) pulses at high intensities (ps1 – $E_L = 0.52$ J, $\tau = 1$ ps, $\varphi = 0°$, FP = 0 μm; sns1 – $E_L = 0.56$ J, $\tau = 0.5$ ns, $\varphi = 0°$, FP = 0 μm; sns2 – $E_L = 0.49$ J, $\tau = 0.5$ ns, $\varphi = 0°$, FP = −400 μm).

similar for each element), about 3 mm long, and with a surprisingly high lifetime measured up to ~20 ns, at least. However, it does not mean that these ions must be the fastest one. Some available interferogram pictures suggest the existence of two additional side groups of ions with the preferred directions ± ~40° with regard to the target normal, the parameters of which may be even higher.

CONCLUSION

Generally, it is accepted that the majority of ions from laser-produced plasma is emitted along the target normal. This is based on the planar target, the geometry of which tends to form narrow jets of high-energy ions with the high charge states. However, more detailed systematic measurements proved that especially at high laser power densities and with the significant participation of non-linear processes, other preferred directions or smaller secondary maxima can appear. A very important role is played by the laser beam interaction with pre-formed laser plasma, as well as the focus setting, and the angle of irradiation of target surface, especially at high laser intensities. Planar geometry of the target tends to prefer the emission (acceleration) of ions perpendicularly to the target due to the ambipolar electric field of escaping thermal or fast electrons, while the radial component of the ponderomotive or thermo-kinetic forces drives them radially with regard to the laser beam axis.

ACKNOWLEDGMENT

This contribution is dedicated to the memory of our colleague E. Woryna who started this work a few years ago, but he did not manage to finish it. M. Lásková is acknowledged for the technical help. The grant agency of the Academy of Sciences of the Czech Republic kindly supported this work (project number IAA 100100715). The support of the 5th National Committee of INFN to the platone experiment is also acknowledged.

REFERENCES

Badziak, J. (2007). Laser-driven generation of fast particles. *Opto-Electr. Rev.* **15**, 1–12.

Badziak, J., Glowacz, S., Jablonski, S., Parys, P., Wolowski, J., Hora, H., Krása, J., Láska, L. & Rohlena, K. (2004). Production of ultrahigh ion current densities at skin-layer subrelativistic laser-plasma interaction. *Plasma Phys. Contr. Fusion* **46**, B541–B555.

Badziak, J., Hora, H., Woryna, E., Jablonski, S., Láska, L., Parys, P., Rohlena, K. & Wolowski, J. (2003). Experimental evidence of differences in properties of fast ion fluxes from short-pulse and long-pulse laser-plasma interactions. *Phys. Lett. A* **315**, 452–457.

Badziak, J., Kasperczuk, A., Parys, P., Pisarczyk, T., Rosinski, M., Ryć, L., Wolowski, J., Jablonski, S., Suchanska, R., Krouský, E., Láska, L., Mašek, K., Pfeifer, M., Ullschmied, J., Dareshwar, L.J., Foldes, I., Torrisi, L. & Pisarczyk, P. (2007). Production of high-current heavy ion jets at the short-wavelength subnanosecond laser-solid interaction. *Appl. Phys. Lett.* **91**, 081502.

Basov, N.G., Getz, K., Maksimchouk, A.M., Mikhailov, Y.A., Rode, A.V., Sklizkov, G.V., Fedotov, S.I., Ferster, E. & Hora, H. (1987). Investigation of fast ion generation in a laser plasma by X-ray-line radiation. *Zh. Eksp. Teor. Fiz.* **92**, 1299–1305.

Buttini, E., Thum-Jager, A. & Rohr, K. (1998). The mass dependence of the jet formation in laser-produced particle beams. *J. Phys. D – Appl. Phys.* **31**, 2165–2169.

Chvojka, M., Králiková, B., Krása, J., Láska, L., Mašek, K., Rohlena, K., Skála, J., Mroz, W., Parys, P., Wolowski, J. & Woryna, E. (1994). Ion generation from Al-laser-produced plasma. *Czech. J. Phys.* **44**, 851–864.

Ehler, A.W. (1975). High-energy ions from a CO_2 laser-produced plasma. *J. Appl. Phys.* **46**, 2464–2467.

Gitomer, S.J., Jones, R.D., Begay, F., Ehler, A.W., Kepphart, J.F. & Kristal, R. (1986). Fast ions and hot electrons in the laser-plasma interactions. *Phys. Fluids* **29**, 2679–2688.

Haseroth, H. & Hora, H. (1996). Physical mechanisms leading to high currents of highly charged ions in laser-driven ion sources. *Laser Part. Beams* **14**, 393–438.

Hauser, T., Scheid, W. & Hora, H. (1992). Theory of ions emitted from a plasma by relativistic self-focusing of laser beams. *Phys. Rev. A* **45**, 1278–1281.

Hora, H. (1969). Self-focusing of laser beams in a plasma by ponderomotive forces. *Z. Physik* **226**, 156–159.

Hora, H. (1975). Theory of relativistic self-focusing of laser radiation in plasma. *J. Opt. Soc. Am.* **65**, 882–886.

Jungwirth, K. (2005). Recent highlights of the PALS research program. *Laser Part. Beams* **23**, 177–182.

Jungwirth, K., Cejnarová, A., Juha, L., Králiková, B., Krása, J., Krouský, E., Krupièková, P., Láska, L., Mašek, K., Mocek, T., Pfeifer, M., Präg, A., Renner, O., Rohlena, K., Rus, B., Skála, J., Straka, P. & Ullschmied, J. (2001). The Prague Asterix Laser System (PALS). *Phys. Plasmas* **8**, 2495–2501.

KASPERCZUK, A., PISARCZYK, T., BORODZIUK, S., ULLSCHMIED, J., KROUSKY, E., MASEK, K., ROHLENA, K., SKALA, J. & HORA, H. (2006). Stable dense plasma jets produced at laser power densities around 10^{14} W/cm^2. *Phys. Plasmas* **13**, 062704.

KASPERCZUK, A., PISARCZYK, T., BORODZIUK, S., ULLSCHMIED, J., KROUSKY, E., MASEK, K., PFEIFER, M., ROHLENA, K., SKALA, J. & PISARCZYK, P. (2007). Interferometric investigations of influence of target irradiation on the parameters of laser-produced plasma jets. *Laser Part. Beams* **25**, 425–433.

KASPERCZUK, A., PISARCZYK, T., KALAL, M., MARTINKOVÁ, M., ULLSCHMIED, J., KROUSKY, E., MASEK, K., PFEIFER, M., ROHLENA, K., SKALA, J. & PISARCZYK, P. (2008). PALS laser energy transfer into solid targets and its dependence on the lens focal point position with respect to the target surface. *Laser Part. Beams* **26**, 189–196.

KELLY, R. & DREYFUS, R.W. (1998). On the effect of Knudsen-layer formation on studies of vaporazation, sputtering, and desorption. *Surf. Sci.* **198**, 263–276.

KRÁSA, J., JUNGWIRTH, K., KROUSKÝ, E., LÁSKA, L., ROHLENA, K., PFEIFER, M., ULLSCHMIED, J. & VELYHAN, A. (2007). Temperature and centre-of-mass energy of ions emitted by laser-produced polyethylene plasma. *Plasma Phys. Contr. Fusion* **49**, 1649–1659.

KRÁSA, J., JUNGWIRTH, K., KROUSKÝ, E., LÁSKA, L., ROHLENA, K., ULLSCHMIED, J. & VELYHAN, A. (2008). Analysis of time-of-flight spectra of ions emitted from laser-generated plasmas. *Radiat. Eff. Defects Solids* **163**.

KRÁSA, J., LÁSKA, L., ROHLENA, K., PFEIFER, M., SKÁLA, J., KRÁLIKOVÁ, B., STRAKA, P., WORYNA, E. & WOLOWSKI, J. (1999). The effect of laser-produced plasma expansion on the ion population. *Appl. Phys. Lett*. **75**, 2539–2541.

KRUSHELNIK, K., CLARK, E.L., BEG, F.N., DANGOR, A.E., NAJMUDIN, Z., NORREYS, P.A., WEI, M. & ZEPF, M. (2005). High intensity laser-plasma sources of ions-physics and future applications. *Plasma Phys. Contr. Fusion* **47**, B451–B463.

KUMAR, A., GUPTA, M.K. & SHARMA, R.P. (2006). Effect of ultra intense laser pulse on the propagation of electron plasma wave in relativistic and ponderomotive regime and particle acceleration. *Laser Part. Beams* **24**, 403–409.

LÁSKA, L., BADZIAK, J., BOODY, F.P., GAMMINO, S., HORA, H., JUNGWIRTH, K., KRÁSA, J., PARYS, P., PFEIFER, M., ROHLENA, K., TORRISI, L., ULLSCHMID, J., WOLOWSKI, J. & WORYNA, E. (2003). Generation of multiply charged ions at low and high laser-power densities. *Plasma Phys. Contr. Fusion* **45**, 585–599.

LÁSKA, L., BADZIAK, J., BOODY, F.P., GAMMINO, S., JUNGWIRTH, K., KRÁSA, J., KROUSKÝ, E., PARYS, P., PFEIFER, M., ROHLENA, K., RYĆ, L., SKÁLA, J., TORRISI, L., ULLSCHMIED, J. & WOLOWSKI, J. (2007*a*). Factors influencing parameters of laser ion sources. *Laser Part. Beams* **25**, 199–205.

LÁSKA, L., BADZIAK, J., BOODY, F.P., GAMMINO, S., JUNGWIRTH, K., KRÁSA, J., KROUSKÝ, E., PARYS, P., PFEIFER, M., ROHLENA, K., RYĆ, L., SKÁLA, J., TORRISI, L., ULLSCHMIED, J. & WOLOWSKI, J. (2007*b*). The influence of an intense laser beam interaction with preformed plasma on the characteristics of emitted ion streams. *Laser Part. Beams* **25**, 549–556.

LÁSKA, L., JUNGWIRTH, K., KRÁLIKOVÁ, B., KRÁSA, J., PFEIFER, M., ROHLENA, K., SKÁLA, J., ULLSCHMIED, J., GAMMINO, S., TORRISI, L., BOODY, F.P., BADZIAK, J., PARYS, P., WOLOWSKI, J. & WORYNA, E. (2002*a*). Generation of Ta ions at high laser-power densities. *Czech. J. Phys*. **52**, 283–291.

LÁSKA, L., JUNGWIRTH, K., KRÁLIKOVÁ, B., KRÁSA, J., PFEIFER, M., ROHLENA, K., SKÁLA, J., ULLSCHMIED, J., BADZIAK, J., PARYS, P., WOLOWSKI, J., WORYNA, E., TORRISI, L., GAMMINO, S. & BOODY, F.P. (2004*a*). Charge-energy distribution of Ta ions from plasmas produced by 1ω and 3ω frequencies of a high-power iodine laser. *Rev. Sci. Instrum*. **75**, 1588–1591.

LÁSKA, L., JUNGWIRTH, K., KRÁSA, J., KROUSKÝ, E., PFEIFER, M., ROHLENA, K., SKÁLA, J., ULLSCHMIED, J., VELYHAN, A., KUBEŠ, P., BADZIAK, J., PARYS, P., ROSINSKI, M., RYC, L. & WOLOWSKI, J. (2006). Experimental studies of interaction of intense long laser pulse with a laser-created Ta plasma. *Czech. J. Phys*., B506–B514.

LÁSKA, L., JUNGWIRTH, K., KRÁSA, J., PFEIFER, M., ROHLENA, K. & ULLSCHMIED, J. (2005*b*). The effect of pre-plasma and self-focusing on characteristics of laser produced ions. *Czech. J. Phys*. **55**, 691–699.

LÁSKA, L., JUNGWIRTH, K., KRÁSA, J., PFEIFER, M., ROHLENA, K., ULLSCHMIED, J., BADZIAK, J., PARYS, P., WOLOWSKI, J., BOODY, F.P., GAMMINO, S. & TORRISI, L. (2004*b*). Generation of extreme high laser intensities in plasma. *Czech. J. Phys*. **54**, C370–C377.

LÁSKA, L., JUNGWIRTH, K., KRÁSA, J., PFEIFER, M., ROHLENA, K., ULLSCHMIED, J., BADZIAK, J., PARYS, P., WOLOWSKI, J., GAMMINO, S., TORRISI, L. & BOODY, F.P. (2005*a*). Charge-state and energy enhancement of laser-produced ions due to nonlinear processes in preformed plasma. *Appl. Phys. Lett*. **86**, 081502.

LÁSKA, L., KRÁSA, J., MAŠEK, K., PFEIFER, M., KRÁLIKOVÁ, B., MOCEK, T., SKÁLA, J., STRAKA, P., TRENDA, P., ROHLENA, K., WORYNA, E., FARNY, J., PARYS, P., WOLOWSKI, J., MROZ, W., SHUMSHUROV, A., SHARKOV, B., COLLIER, J., LANGBEIN, K. & HASEROTH, H. (1996). Iodine laser production of highly charged Ta ions. *Czech. J. Phys*. **46**, 1099–1115.

LÁSKA, L., KRÁSA, J., PFEIFER, M., ROHLENA, K., GAMMINO, S., TORRISI, L., ANDÒ, L. & CIAVOLA, G. (2002*b*). Angular distribution of ions emitted from Nd:YAG laser-produced plasma. *Rev. Sci. Instrum*. **73**, 654–658.

LÁSKA, L., MAŠEK, K., KRÁLIKOVÁ, B., KRÁSA, J., SKÁLA, J., ROHLENA, K., WORYNA, E., WOLOWSKI, J., LANGBEIN, K. & HASEROTH, H. (1994). Highly-charged Ta ions produced by the photo dissociation iodine laser with subnanosecond pulses. *Appl. Phys. Lett*. **65**, 691–693.

LÁSKA, L., RYC, L., BADZIAK, J., BOODY, F.P., GAMMINO, S., JUNGWIRTH, K., KRASA, J., KROUSKY, E., MEZZASALMA, A., PARYS, P., PFEIFER, M., ROHLENA, K., TORRISI, L., ULLSCHMIED, J. & WOLOWSKI, J. (2005*c*). Correlation of highly charged ion and X-ray emissions from the laser-produced plasma in the presence of non-linear phenomena. *Rad. Eff. Def. Solids* **160**, 557–566.

LORUSSO, A., KRÁSA, J., ROHLENA, K., NASSISI, V., BELLONI, F. & DORIA, D. (2005). Charge losses in expanding plasma created by an XeCl laser. *Appl. Phys. Lett.* **86**, 081501.

MRÓZ, W., PARYS, P., WOLOWSKI, J., WORYNA, E., KRÁLIKOVÁ, B., KRÁSA, J., LÁSKA, L., MAŠEK, K., SKÁLA, J. & ROHLENA, K. (1994). Investigation of iodine laser interaction of intensities $I\lambda^2 \sim 10^{13}-10^{15}$ W cm^{-2} μM^2 with aluminum targets. *Laser Part. Beams* **12**, 421–433.

NICOLAÏ, PH., TIKHONCHUK, V.T., KASPERCZUK, A., PISARCZYK, T., BORODZIUK, S., ROHLENA, K. & ULLSCHMIED, J. (2006). Plasma jets produced in a single laser beam interaction with a planar target. *Phys. Plasmas* **13**, 062701.

Picciotto, A., Krása, J., Láska, L., Rohlena, K., Torrisi, L., Gammino, S., Mezzasalma, A.M. & Caridi, F. (2006). Plasma temperature and ion current analysis of gold ablation at different laser power rates. *Nucl. Instrum. Meth. Phys. Res. B* **247**, 261–267.

Rohlena, K., Králiková, B., Krása, J., Láska, L., Mašek, K., Pfeifer, M., Skála, J., Parys, P., Wolowski, J., Woryna, E., Farny, J., Mroz, W., Roudskoy, I., Shamaev, O., Sharkov, B., Shumshurov, A., Bryunetkin, B.A., Haseroth, H., Collier, J., Kuttenberger, A., Langbein, K. & Kugker, H. (1996). Ion production by lasers using high-power densities in a near infrared region. *Laser Part. Beams* **14**, 335–345.

Roudskoy, I.V. (1996). General features of highly charged ion generation in laser-produced plasmas. *Laser Part. Beams* **14**, 369–384.

Rowlands, T.P. (2006). General foundation for the nonlinear ponderomotive four-force in laser-plasma interactions. *Laser Part. Beams* **24**, 475–493.

Rus, B., Zeitoun, P., Mocek, T., Sebban, S., Kalal, M., Demir, A., Jamelot, G., Klisnick, A., Kralikova, B., Skala, J. & Tallents, G.J. (1997). Investigation of Zn and Cu prepulse plasmas relevant to collisional excitation X-ray lasers. *Laser Phys. Rev. A* **56**, 4229–4241.

Schaumann, G., Schollmeier, M.S., Rodriguez-Prieto, G., Blazevic, A., Brambrink, E., Geissel, M., Korostiy, S., Pirzadeh, P., Roth, M., Rosmej, F.B., Faenov, A.Ya., Pikuz, T.A., Tsigutkin, K., Maron, Y., Tahir, N.A. & Hoffmann, D.H.H. (2005). High energy heavy ion jets emerging from laser plasma generated by long pulse laser beams from the NHELIX laser system at GSI. *Laser Part. Beams* **23**, 503–512.

Stritzker, B., Pospieszczyk, A. & Tagle, J.A. (1981). Measurement of lattice temperature of silicon during pulsed laser annealing. *Phys. Rev. Lett*. **47**, 356–358.

Thum, A., Rupp, A. & Rohr, K. (1994). 2-component structure in the angular emission of a laser-produced Ta plasma. *J. Phys. D – Appl. Phys*. **27**, 1791–1794.

Thum-Jager, A. & Rohr, K. (1999). Angular emission distributions of neutrals and ions in laser ablated particle beams. *J. Phys. D – Appl. Phys*. **32**, 2827–2831.

Torrisi, L., Andò, L., Ciavola, G., Gammino, S. & Barnà, A. (2001*b*). Angular distribution of ejected atoms from Nd:YAG laser irradiating metals. *Rev. Sci. Instrum*. **72**, 68–72.

Torrisi, L., Andò, L., Gammino, S., Krása, J. & Láska, L. (2001*a*). Ion and neutral emission from pulsed laser irradiation of metals. *Nucl. Instrum. Meth. Phys. Res. B* **184**, 327–336.

Torrisi, L., Ciavola, G., Gammino, S., Andò, L., Barnà, A., Láska, L. & Krása, J. (2000). Metallic etching by high power Nd:Yttrium-aluminum-garnet pulsed laser irradiation. *Rev. Sci. Instrum*. **71**, 4330–4334.

Vanrompay, P.A., Nantel, M. & Pronko, P.P. (1998). Pulse-contrast effects on energy distributions of C^{1+} to C^{4+} ions for high-intensity 100-Fs laser-ablation plasmas. *Appl. Surf. Sci.*, **127–129**, 1023–1028.

Wolowski, J., Badziak, J., Boody, F.P., Hora, H., Hnatowicz, V., Jungwirth, K., Krása, J., Láska, L., Parys, P., Peøina, V., Pfeifer, M., Rohlena, K., Ryc, L., Ullschmied, J. & Woryna, E. (2002*a*). Fast ion emission from the plasma produced by the PALS laser system. *Plasma Phys. Cont. Fusion* **44**, 1277–1283.

Wolowski, J., Badziak, J., Boody, F.P., Czarnecka, A., Gammino, S., Jablonski, S., Krása, J., Láska, L., Parys, P., Rohlena, K., Rosinski, M., Ryc, L., Torrisi, L. & Ullschmied, J. (2006). Generation of fast highly charged ions in laser-plasma interaction. *Plasma Phys. Contr. Fusion* **48**, B475–B482.

Wolowski, J., Badziak, J., Boody, F.P., Gammino, S., Hora, H., Jungwirth, K., Krása, J., Láska, L., Parys, P., Pfeifer, M., Rohlena, K., Szydlowski, A., Torrisi, L., Ullschmied, J. & Woryna, E. (2003). Characteristics of ion emission from plasma produced by high-energy short-wavelength (438 nm) laser radiation. *Plasma Phys. Contr. Fusion* **45**, 1087–1093.

Wolowski, J., Badziak, J., Czarnecka, A., Parys, P., Pisarek, M., Rosinski, M., Turan, R. & Yerci, S. (2007). Application of pulsed laser deposition and laser-induced ion implantation for formation of semiconductor nano-crystallites. *Laser Part. Beams* **25**, 65–69.

Wolowski, J., Badziak, J., Krása, J., Láska, L., Parys, P., Rohlena, K. & Woryna, E. (2002*b*). Investigations of ion emission from plasma produced by a high-power 1 ps laser pulse. *Plasma Sources Sci. Technol*. **11**, A173–A177.

Woryna, E., Badziak, J., Krasa, J., Laska, L., Makowski, J., Parys, P., Rohlena, K., Vankov, A.B., & Wolowski, J. (2001). Dependence of parameters of Au plasmas generated by sub-nanosecond and picosecond laser pulses. Warsaw, Poland: IPPLM.

Woryna, E., Parys, P., Wolowski, J. & Mróz, W. (1996*b*). Corpuscular diagnostics and processing methods applied in investigations of laser-produced plasma as a source of highly ionized ions. *Laser Part. Beams* **14**, 293–321.

Woryna, E., Parys, P., Wolowski, J., Krása, J., Láska, L., Králiková, B., Skála, J. & Rohlena, K. (1999). Angular distribution of ions from laser produced plasma. *Laser Part. Beams* **17**, 307–312.

Woryna, E., Parys, P., Wolowski, J., Láska, L., Krása, J., Mašek, K., Pfeifer, M., Králiková, B., Skála, J., Straka, P. & Rohlena, K. (1996*a*). Au^{49+}, Pb^{50+}, and Ta^{48+} ions from laser-produced plasmas. *Appl. Phys. Lett*. **69**, 1547–1549.